Study on low cycle fatigue crack growth property based on stress triaxiality factor

Takehisa Yamada[1*] and Youichi Yamashita[1]

[1]1, Shin-Nakahara-Cho, Isogo-Ku, Yokohama 235-8501 Japan, IHI Corporation

[*]takehisa_yamada@ihi.co.jp

Keywords: Nonlinear Fracture Mechanics, Fatigue Crack Growth, J-integral Range, Stress Triaxiality Factor

Abstract. Evaluation method for fatigue crack growth rate under large scale yielding condition was investigated based on ΔJ. Low cycle fatigue crack growth tests were carried out using CT specimens of SM400B steel with some sizes of plate thickness. As the results, plate thickness effect appeared in the relationships between fatigue crack growth rate and ΔJ calculated by Merkle and Corten's conventional equation. Moreover, P-V curves and ΔJ could be analytically computed employing modified cyclic stress-strain curves as the constitutive equation for FE-analyses. It was found that P-V curves employed to calculate the experimental ΔJ were approximately coincident by taking account of stress triaxiality factor at the crack tip obtained from the above FE-analyses in addition to plate thickness. Therefore, the conventional equation of ΔJ was modified by introducing the stress triaxiality factor. Fatigue crack growth rate could be evaluated by the modified ΔJ without depending on the size of plate thickness.

Introduction

For fatigue crack growth under small yielding condition, the evaluation method based on linear fracture mechanics has been established. However, in the case that the fatigue crack grows with fully plastic deformation, the method based on linear fracture mechanics might lose the validity. For the evaluation on fatigue crack growth under elastic-plastic deformation, it has been shown that nonlinear fracture mechanics parameter is effective [1,2]. Dowling and Begley [1] experimentally indicated that J-integral range ΔJ is the effective parameter.

On the other hand, the J-integral can be the dominant parameter describing stress-strain fields at crack tip when the stress fields agree with HRR fields [3,4]. However, from recent analytical investigations [5,6], it has been reported that there are some cases that the stress fields at crack tip do not agree with HRR fields. It is considered that the disagreement comes from the effect of the plastic constraint at the crack tip due to the difference of specimen thickness, crack geometry and deformation level. And the second parameter such as Q parameter [7,8], which corresponds to the stress triaxiality at the crack tip, has been proposed and also employed as the parameter expressing the plastic constraint at crack tip. For fracture toughness evaluation under large scale yielding condition, some applications of plastic constraint parameter to the J-integral have been reported [9,10]. Since ΔJ is the parameter extending the J-integral, it might be expected that the application of plastic constraint parameter to ΔJ is also significant.

In this study, low cycle fatigue crack growth tests were carried out using CT specimens with some sizes of plate thickness and the effect of plate thickness on fatigue crack growth property under large scale yielding was experimentally obtained. In addition, the analytical method of computing ΔJ by FE-analysis was considered. Furthermore, in order to evaluate fatigue crack growth rate without depending on the size of plate thickness, the possibility of application of plastic constraint parameter to ΔJ was discussed.

Experimental procedure

The material used is SM400B steel in the Japan Industrial Standard. The chemical composition and the mechanical properties are summarized in Table 1 and 2. The specimen geometry is CT specimen and the sizes of plate thickness B are 35, 8 and 3 mm. The rolling direction is perpendicular to the crack growth direction, that is to say L-T direction described in ASTM E399 - 90. Before carrying out low cycle fatigue crack growth tests, fatigue precrack was introduced and side grooves (S.G.) were machined under the conditions described in ASTM E 1820 - 01. Main dimensions of CT specimens used are summarized in Table 3. The configuration of CT specimen is shown in Fig. 1.

The testing machine used is a closed-loop servo hydraulic type. To carry out load line displacement controlling test, cyclic deformation was given to CT specimen by controlling load line displacement V using knife edges. The test frequency was 0.5 Hz. The ranges of V for each specimen are summarized in Table 4. Crack lengths were measured with elastic compliance technique described in ASTM E 1820 - 01. Fatigue crack growth rates da/dN were determined by an incremental polynominal method described in ASTM E 647 – 00.

Table 1 Chemical composition of SM400B steel (wt%).

Material	C	Si	Mn	P	S
SM400B	0.15	0.28	1.02	0.019	0.004

Table 2 Mechanical properties of SM400B steel.

Yield Stress σ_y [MPa]	Tensile Strength σ_u [MPa]	Elongation δ [%]
318	467	37

Table 3 Main dimensions of CT specimens.

Specimen	Width W [mm]	Plate thickness B [mm]	Net thickness between S.G. B_n [mm)]	Initial crack length a_0 [mm]
A		35	28	
B	50	8	6.4	25
C		3	2.5	

Table 4 The ranges of load line displacement for each specimen.

Specimen	Range of V [mm]
A-1	0 - 0.7
B-1	0 - 0.7
B-2	0 - 1.0
C-1	0 - 0.7
C-2	0 - 1.0

ΔJ equation

Extending the J integral equation considering axial load in addition to bending load, which has been proposed by Merkle and Corten [11], experimentally determined equation of ΔJ for CT specimen can be given by the following equation;

$$\Delta J = \frac{1+\eta}{1+\eta^2}\frac{2U^*}{B(W-a)} \tag{1}$$

$$\eta = \frac{\sqrt{2+2\alpha^2}-(1+\alpha)}{1-\alpha}, \qquad \alpha = \frac{a}{W} \tag{2}$$

where W is the specimen width and a is the crack length. B is the plate thickness but is substituted by the net thickness between side grooves B_n. U^* is the area determined by loading portion of load and load line displacement curve (P-V curve) during which the crack could be estimated to be open as shown in Fig. 2.

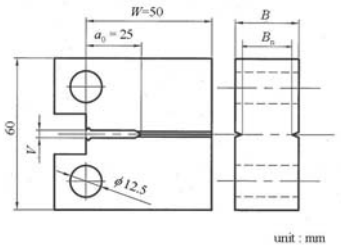

Fig. 1 Configuration of CT specimen.

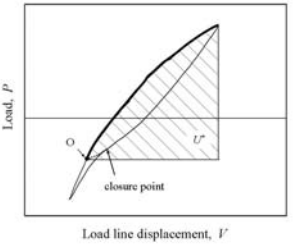

Fig. 2 Definition of U^*.

FE-analyses

Three-dimensional (3-D) and elastic-plastic FE-analyses were performed using the general-purpose FE program, ABAQUS Ver.6.6-3. For example, the 3-D FE model of B = 35 mm is shown in Fig. 3. The FE models were deformed by the imposed displacement D given at the center of pin hole, which is corresponding to V, that is $D = V/2$. And S.G. configurations were modeled.

To analytically compute P-V curves and stress-strain fields at crack tip, the stress-strain relationship for FE-analyses was determined by the following procedure. Cyclic stress-strain curve is experimentally obtained from strain controlled cyclic loading tests as shown in Fig. 4(a) and can be represented by the following Ramberg-Osgood power law relationship;

$$\frac{\varepsilon}{\varepsilon_y} = \frac{\sigma}{\sigma_y} + \alpha\left(\frac{\sigma}{\sigma_y}\right)^n \tag{3}$$

where σ is stress and ε is strain. σ_y and ε_y denote yield stress and strain, respectively. n is the strain hardening exponent and α is the material constant. ΔJ can be experimentally obtained using the area determined from P-V curve (See Fig. 2). On the other hand, the J-integral is analytically obtained using a domain integral within ABAQUS program. Once P-V curve equivalent to the experimental loading portion can be analytically obtained, the J-integral obtained by FE-analysis could be assumed as ΔJ. Therefore, each parameter in Eq. 3 was varied to be coincident with the loading portions of each hysteresis loop for each strain range so that the P-V curve equivalent to the bold curve in Fig. 2 can be obtained in monotonically loading by FE-analysis. Modified Ramberg-Osgood power law relationship was shown in Fig. 4(b). Where σ_y and ε_y were the double of the corresponding values in Fig. 4(a) and n = 9.0, α = 0.9. In this study, the stress-strain relationship obtained by the above procedure was used as the constitutive equation for FE-analyses.

Experimental results

Typical examples of P-V curves (B = 35 and 3 mm) are shown in Fig. 5. The inflection points of P-V curves might be considered to be crack closure points as shown in Fig. 2. It is found that the maximum load decreases and the quantity of crack closure increases with increasing number of cycles N. Fig. 6 shows the relationships between da/dN and ΔJ. The difference between the ranges of load line displacement for the specimens with the same plate thickness seems to be little. Except for accelerating region of da/dN found at $\Delta J > 10^5$ N/m for specimen A-1, fatigue crack growth rate for

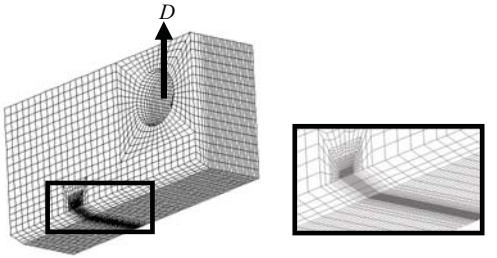

Fig. 3 Example of 3-D FE model (B = 35 mm).

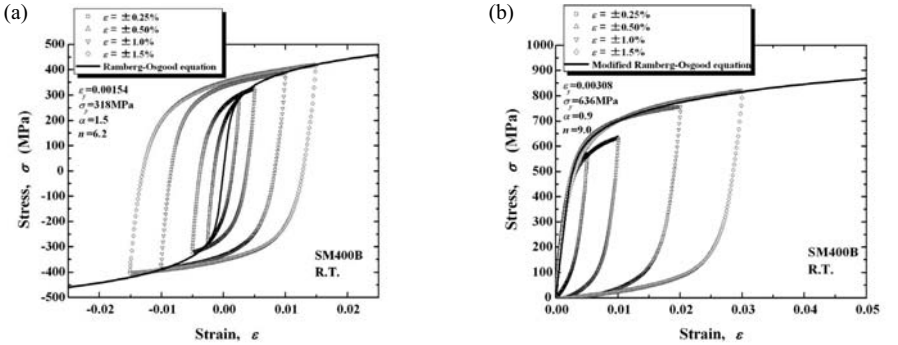

Fig. 4 Stress-strain relationship: (a) cyclic stress-strain curve obtained from strain controlled cyclic loading tests; (b) stress-strain curve used as the constitutive equation for FEM analyses.

each plate thickness can be represented by the following simple power relationship;

$$\frac{da}{dN} = C_j(\Delta J)^{m_j} \tag{4}$$

where C_j and m_j are constants. Theses relationships do not agree with each plate thickness and fatigue crack growth rate becomes larger as the plate thickness becomes smaller. Therefore, the unique relationship between da/dN and ΔJ without depending on plate thickness can not be obtained by ΔJ equation given in Eq.1.

Analytical results

Figure 7 shows the examples of P-V curves obtained by FE-analyses with experimental results when the crack length is 28 mm. Theses analytical results are the ones of small strain analyses. Experimental P-V curves are plotted with shifting the point equivalent to point O in Fig. 2 to the origin. Analytical and experimental values of ΔJ are also shown in Fig. 7 and the former are the values at the center of the plate thickness. It seems that the analytical results depict the curves nearly equal to experimental results for each specimen. Analytical ΔJ of specimen A-1 is almost close to the experimental value and the error is 13%. But, for specimen B-2 and C-2, the errors are comparatively large. The reason is that the experimental load line displacement is smaller than FE-analysis due to crack closure. To analyze the deformation entirely equal to the experimental result, it is necessary to input the imposed displacement calculated by subtracting the quantity of crack closure. In addition, the configurations of crack front were modeled as the straight lines for simplicity. However, in fact, the configurations of fatigue crack front are not straight, which can be verified from the observations

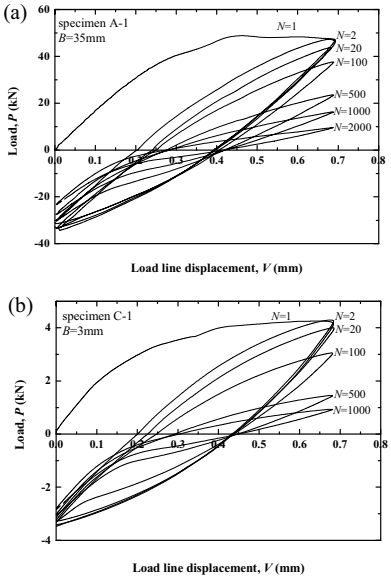

Fig. 5 Typical examples of *P-V* curves: (a) specimen A-1 and (b) specimen C-1.

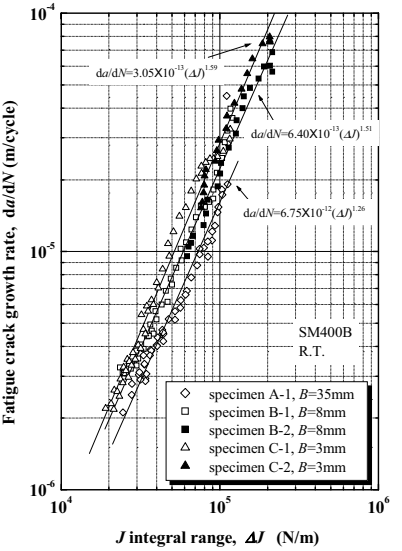

Fig. 6 Relationships between d*a*/d*N* and ΔJ for CT specimens.

of fracture surfaces, and the difference of the configuration is assumed to be one of the causes of the errors between analytical and the experimental results. Though there are disagreements in some cases, it is thought to be possible to compute *P-V* curves and ΔJ with tolerable accuracy by FE-analyses.

Discussions

The effect of plate thickness on P-V curves

The plate thickness *B* and the ligament length *W-a* in Eq. 1 are considered to be the factors to give ΔJ without depending on the remaining cross-section area. Fig. 8 shows *P-V* curves for each plate thickness when *V* is 0 to 0.7 mm and the values of d*a*/d*N* are approximately 1.25×10^{-5} m/cycle. These *P-V* curves are plotted with locating the point equivalent to point O in Fig.2 at the origin as well as Fig. 7. Open marks show the cases that *P* are divided by the remaining cross-section area $B_n \times (W\text{-}a)$. It is found that *P-V* curves divided by $B_n \times (W\text{-}a)$ are different from each plate thickness and the area determined by the *P-V* curve is larger with increase of plate thickness. Since ΔJ is directly influenced by the area, it could be considered that the effect of plate thickness on the relationships between d*a*/d*N* and ΔJ as shown in Fig. 6 results. In other words, there is a possibility that ΔJ equation such as Eq. 1 is not enough to consider the effect of plate thickness.

Noticing the stress fields at crack tip, crack opening stress distributions depend on specimen thickness, crack geometry and deformation level [5,6] and it is thought of as the influence of plastic constraint. As the useful parameter to quantify the out-of plane constraint effect, there is a stress triaxiality factor S_m/S_e defined below;

$$\frac{S_m}{S_e} = \frac{(\sigma_1 + \sigma_2 + \sigma_3)/3}{\sqrt{\frac{1}{2}\left\{(\sigma_1 - \sigma_2)^2 + (\sigma_2 - \sigma_3)^2 + (\sigma_3 - \sigma_1)^2\right\}}} \tag{5}$$

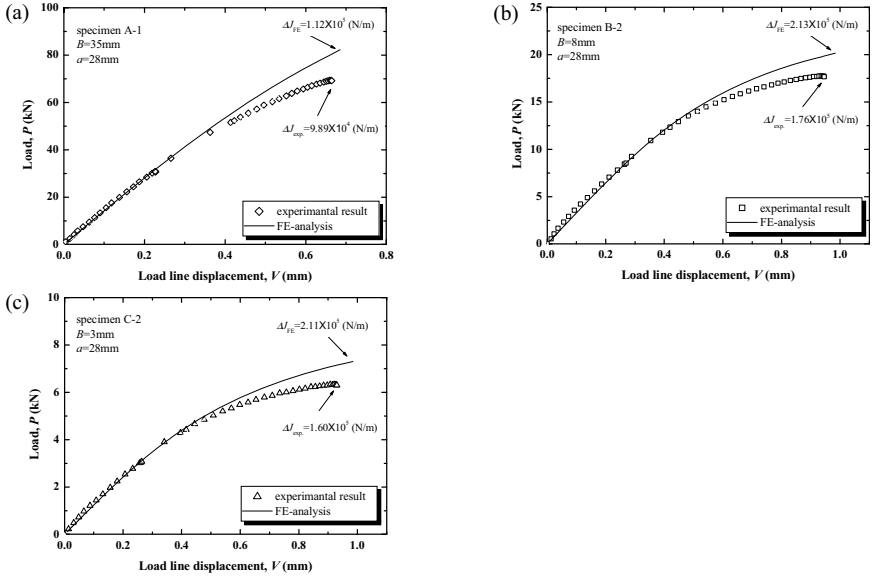

Fig. 7 Experimental and analytical *P-V* curves: (a) specimen A-1, (b) specimen B-2 and (c) specimen C-2, when the crack length is 28 mm.

where σ_1, σ_2 and σ_3 denote principle stress components and S_e denotes von-Mises equivalent stress. Assuming that the relationships among each stress at crack tip can be expressed using the foregoing analytical method, stress triaxiality factors at the center of plate thickness in the final stage of deformation can be determined by FE-analyses. For example, the distributions of crack opening stress $\sigma_{\theta\theta}$ is shown in Fig. 9, when the crack length is 28 mm and D is 0.35 mm, which is corresponding to V = 0.7 mm. $\sigma_{\theta\theta}$ is normalized by the yield stress σ_y used for FE-analysis and the distance from the crack tip r is normalized by ΔJ computed by FE-analysis and the σ_y respectively. $\sigma_{\theta\theta}$ is the value at the center of plate thickness. Regarding the distinct region at the crack tip between small strain and finite strain analysis as the fracture process zone, S_m/S_e was determined at the location outside of the zone, that is to say, r is approximately $\Delta J/\sigma_y$. Half marks in Fig. 8 show the cases that P are divided by the S_m/S_e in addition to the remaining cross-section area. Though there is a slight difference due to the quantity of crack closure among each plate thickness, the *P-V* curves taking account of S_m/S_e are approximately coincident without depending on plate thickness.

Relationships between da/dN and ΔJ taking account of S_m/S_e

Since *P-V* curves without depending on plate thickness are obtained by taking account of S_m/S_e as described above, it is expected that ΔJ without depending on plate thickness is also obtained by employing S_m/S_e to the conventional evaluation equation. Therefore, ΔJ equation is modified such as the following equation by introducing S_m/S_e;

$$\Delta J' = \frac{1+\eta}{1+\eta^2}\frac{2U^*}{B(W-a)\dfrac{S_m}{S_e}} = \Delta J \Big/ \frac{S_m}{S_e} \tag{6}$$

S_m/S_e is considered to be variable with depending on a. Fig. 10 shows the relationships between S_m/S_e and a in the case that D is 0.35 mm. It is pointed out that S_m/S_e are different from each plate

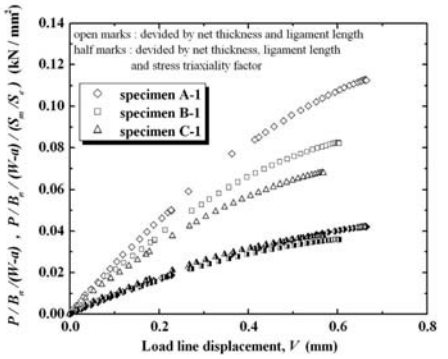

Fig. 8 Load versus load line displacement curves when V is 0 to 0.7 mm and the values of da/dN are approximately 1.25×10^{-5} m/cycle.

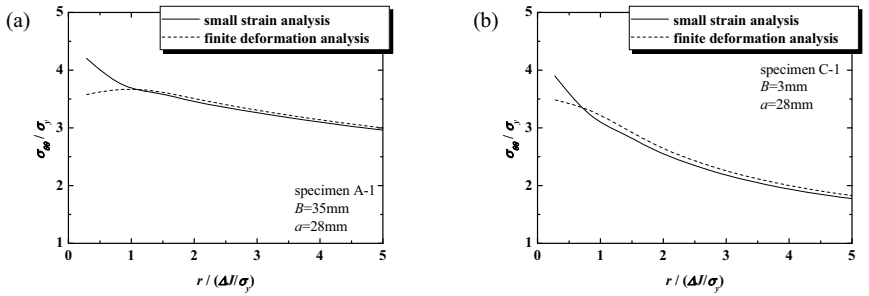

Fig. 9 Crack opening stress distribution at crack tip: (a) specimen A-1 and (c) specimen C-1, when the crack length is 28 mm and D is 0.35 mm.

thickness. S_m/S_e of specimen A-1 decreases with increase of a and S_m/S_e of specimen B-1 and C-1 slightly increase. Approximating these relationships using linear expression and employing S_m/S_e for each crack length to Eq. 6, the relationships between da/dN and $\Delta J'$ is shown as Fig. 11. It is found that da/dN is evaluated by $\Delta J'$ without depending on plate thickness except accelerating region found for specimen A-1 and represented by the following power relationship uniquely;

$$\frac{\mathrm{d}a}{\mathrm{d}N}=1.45\times10^{-12}(\Delta J)^{1.54} \tag{7}$$

Employing the plastic constraint parameter to ΔJ might be effective to obtain the relationship between da/dN and $\Delta J'$ without depending on not only plate thickness but also crack geometry and loading type.

Summary

Fatigue crack growth tests under large scale yielding condition were carried out using CT specimens of SM400B steel with some sizes of plate thickness. It was found that there was the effect of plate thickness on low cycle fatigue crack growth properties, which are the relationships between da/dN and ΔJ. Focusing on stress triaxiality factor as constraint parameter at the crack tip, the possibility for applying stress triaxiality factor to ΔJ was investigated. Obtained results are as follows;

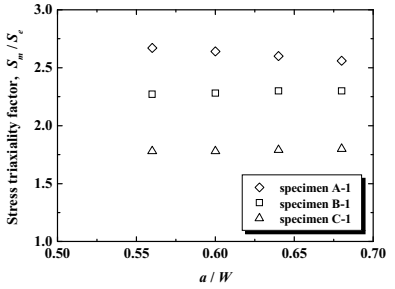

Fig. 10 Relationships between stress triaxiality factor and the ratio of crack length to specimen width a/W.

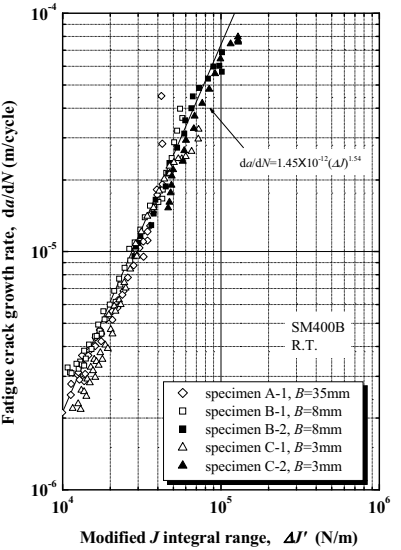

Fig. 11 Relationships between da/dN and $\Delta J'$.

1. In the case of employing conventional ΔJ equation under large scale yielding condition, the relationships between da/dN and ΔJ were different from each plate thickness and the decrease of plate thickness gave the increase of da/dN.
2. Employing the stress-strain relationship determined to be coincident with the loading portions obtained from cyclic loading tests as the constitutive equation for FE-analyses, which is shown in Fig. 4(b), P-V curves and ΔJ could be analytically computed with tolerable accuracy.
3. For fatigue crack growth under large scale yielding condition, fatigue crack growth rate could be uniquely evaluated without depending on plate thickness by introducing stress triaxiality factor to conventional ΔJ equation.

References

[1] N. E. Dowling and J. A. Begley: ASTM STP 590, 1976, pp. 82-103.
[2] N. E. Dowling: ASTM STP 601, 1976, pp. 19-32.
[3] J. W. Hutchinson: J. Mech. Phys. Solids, Vol. 16, 1968, pp. 13-31.
[4] J. R. Rice and G. F. Rosengren: J. Mech. Phys. Solids, Vol. 16, 1968, pp. 1-12.
[5] M. Kikuchi : Int. J. Fracture, Vol. 58, 1992, pp. 273-283.
[6] M. Kikuchi : Int. J. Pressure Vessel Piping, Vol. 63, 1995, pp. 315-326.
[7] N. P. O'Dowd and C. F. Shih: J. Mech. Phys. Solids, Vol. 39, No. 8, 1991, pp. 989-1015.
[8] N. P. O'Dowd and C. F. Shih: J. Mech. Phys. Solids, Vol. 40, No. 5, 1992, pp. 939-963.
[9] S. Jun: Eng. Fracture Mech., Vol. 44, No. 5, 1993, pp. 789-806.
[10] T. Wang: Eng. Fracture Mech., Vol. 48, No. 2, 1994, pp. 217-230.
[11] J. G. Merkle and H. T. Corten: J. Pressure Vessel Tech., Tran. ASME, 1974, pp. 286-292.